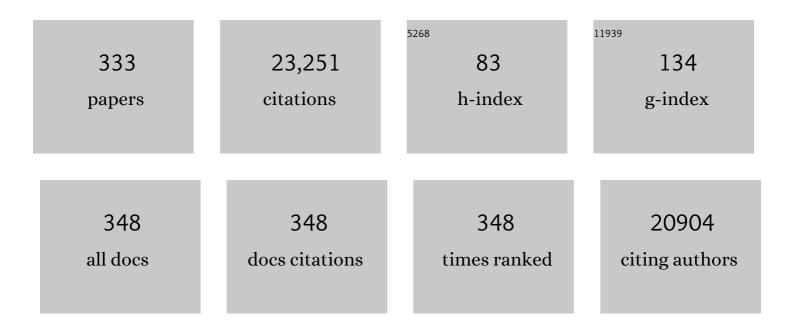
List of Publications by Year in descending order

Source: https://exaly.com/author-pdf/988404/publications.pdf Version: 2024-02-01



| # | Article | IF | CITATIONS |
|----|---|------|-----------|
| 1 | Imaging biomarker roadmap for cancer studies. Nature Reviews Clinical Oncology, 2017, 14, 169-186. | 27.6 | 792 |
| 2 | Hypoxia: Importance in tumor biology, noninvasive measurement by imaging, and value of its measurement in the management of cancer therapy. International Journal of Radiation Biology, 2006, 82, 699-757. | 1.8 | 561 |
| 3 | A novel approach to overcome hypoxic tumor resistance: Cu-ATSM-guided intensity-modulated radiation therapy. International Journal of Radiation Oncology Biology Physics, 2001, 49, 1171-1182. | 0.8 | 410 |
| 4 | ⁸⁹ Zr-DFO-J591 for ImmunoPET of Prostate-Specific Membrane Antigen Expression In Vivo. Journal of Nuclear Medicine, 2010, 51, 1293-1300. | 5.0 | 373 |
| 5 | Standardized methods for the production of high specific-activity zirconium-89. Nuclear Medicine and Biology, 2009, 36, 729-739. | 0.6 | 369 |
| 6 | Copper radionuclides and radiopharmaceuticals in nuclear medicine. Nuclear Medicine and Biology, 1996, 23, 957-980. | 0.6 | 361 |
| 7 | In vivo assessment of tumor hypoxia in lung cancer with 60Cu-ATSM. European Journal of Nuclear Medicine and Molecular Imaging, 2003, 30, 844-850. | 6.4 | 358 |
| 8 | PET imaging with 89Zr: From radiochemistry to the clinic. Nuclear Medicine and Biology, 2013, 40, 3-14. | 0.6 | 338 |
| 9 | Assessing tumor hypoxia in cervical cancer by positron emission tomography with 60Cu-ATSM: Relationship to therapeutic response—a preliminary report. International Journal of Radiation Oncology Biology Physics, 2003, 55, 1233-1238. | 0.8 | 324 |
| 10 | Imaging oxygenation of human tumours. European Radiology, 2007, 17, 861-872. | 4.5 | 304 |
| 11 | Cerenkov Luminescence Imaging of Medical Isotopes. Journal of Nuclear Medicine, 2010, 51, 1123-1130. | 5.0 | 279 |
| 12 | PI3K inhibition results in enhanced estrogen receptor function and dependence in hormone receptor–positive breast cancer. Science Translational Medicine, 2015, 7, 283ra51. | 12.4 | 276 |
| 13 | Glutamine-based PET imaging facilitates enhanced metabolic evaluation of gliomas in vivo. Science Translational Medicine, 2015, 7, 274ra17. | 12.4 | 257 |
| 14 | Copper bis(thiosemicarbazone) complexes as hypoxia imaging agents: structure-activity relationships. Journal of Biological Inorganic Chemistry, 2002, 7, 249-259. | 2.6 | 248 |
| 15 | A Pretargeted PET Imaging Strategy Based on Bioorthogonal Diels–Alder Click Chemistry. Journal of Nuclear Medicine, 2013, 54, 1389-1396. | 5.0 | 247 |
| 16 | Metal complexes as diagnostic tools. Coordination Chemistry Reviews, 1999, 184, 3-66. | 18.8 | 246 |
| 17 | Affinity-based proteomics reveal cancer-specific networks coordinated by Hsp90. Nature Chemical Biology, 2011, 7, 818-826. | 8.0 | 240 |
| 18 | Evaluation of 64Cu-ATSM in vitro and in vivo in a hypoxic tumor model. Journal of Nuclear Medicine, 1999, 40, 177-83. | 5.0 | 236 |

| # | Article | IF | CITATIONS |
|----|---|------|-----------|
| 19 | The epichaperome is an integrated chaperome network that facilitates tumour survival. Nature, 2016, 538, 397-401. | 27.8 | 233 |
| 20 | Assessing Tumor Hypoxia in Cervical Cancer by PET with ⁶⁰ Cu-Labeled Diacetyl-Bis(<i>N</i> ⁴ -Methylthiosemicarbazone). Journal of Nuclear Medicine, 2008, 49, 201-205. | 5.0 | 221 |
| 21 | Cu–ATSM: A radiopharmaceutical for the PET imaging of hypoxia. Dalton Transactions, 2007, , 4893. | 3.3 | 213 |
| 22 | 64Cu-TETA-octreotide as a PET imaging agent for patients with neuroendocrine tumors. Journal of Nuclear Medicine, 2001, 42, 213-21. | 5.0 | 203 |
| 23 | Convection-enhanced delivery for diffuse intrinsic pontine glioma: a single-centre, dose-escalation, phase 1 trial. Lancet Oncology, The, 2018, 19, 1040-1050. | 10.7 | 201 |
| 24 | Click Chemistry and Radiochemistry: The First 10 Years. Bioconjugate Chemistry, 2016, 27, 2791-2807. | 3.6 | 197 |
| 25 | Copper-64-diacetyl-bis(N4-methylthiosemicarbazone): An agent for radiotherapy. Proceedings of the National Academy of Sciences of the United States of America, 2001, 98, 1206-1211. | 7.1 | 192 |
| 26 | Assessment of regional tumor hypoxia using 18F-fluoromisonidazole and 64Cu(II)-diacetyl-bis(N4-methylthiosemicarbazone) positron emission tomography: Comparative study featuring microPET imaging, Po2 probe measurement, autoradiography, and fluorescent microscopy in the R3327-AT and FaDu rat tumor models. International Journal of Radiation Oncology Biology Physics, 2005, 61, 1493-1502. | 0.8 | 183 |
| 27 | An Imaging Comparison of ⁶⁴ Cu-ATSM and ⁶⁰ Cu-ATSM in Cancer of the Uterine Cervix. Journal of Nuclear Medicine, 2008, 49, 1177-1182. | 5.0 | 178 |
| 28 | First-in-Humans Imaging with ⁸⁹ Zr-Df-IAB22M2C Anti-CD8 Minibody in Patients with Solid Malignancies: Preliminary Pharmacokinetics, Biodistribution, and Lesion Targeting. Journal of Nuclear Medicine, 2020, 61, 512-519. | 5.0 | 170 |
| 29 | A practical guide to the construction of radiometallated bioconjugates for positron emission tomography. Dalton Transactions, 2011, 40, 6168. | 3.3 | 169 |
| 30 | Small animal imaging. European Journal of Cancer, 2002, 38, 2173-2188. | 2.8 | 168 |
| 31 | Role of Metalation in the Topoisomerase IIα Inhibition and Antiproliferation Activity of a Series of α-Heterocyclic-N ⁴ -Substituted Thiosemicarbazones and Their Cu(II) Complexes. Journal of Medicinal Chemistry, 2011, 54, 2391-2398. | 6.4 | 168 |
| 32 | CDK9-mediated transcription elongation is required for MYC addiction in hepatocellular carcinoma. Genes and Development, 2014, 28, 1800-1814. | 5.9 | 167 |
| 33 | A Phase I/II Study for Analytic Validation of 89Zr-J591 ImmunoPET as a Molecular Imaging Agent for Metastatic Prostate Cancer. Clinical Cancer Research, 2015, 21, 5277-5285. | 7.0 | 163 |
| 34 | A Novel Technology for the Imaging of Acidic Prostate Tumors by Positron Emission Tomography. Cancer Research, 2009, 69, 4510-4516. | 0.9 | 154 |
| 35 | 1- ¹¹ C-Acetate as a PET Radiopharmaceutical for Imaging Fatty Acid Synthase Expression in Prostate Cancer. Journal of Nuclear Medicine, 2008, 49, 327-334. | 5.0 | 152 |
| 36 | Tumor Hypoxia Detected by Positron Emission Tomography with 60Cu-ATSM as a Predictor of Response and Survival in Patients Undergoing Neoadjuvant Chemoradiotherapy for Rectal Carcinoma: A Pilot Study. Diseases of the Colon and Rectum, 2008, 51, 1641-1648. | 1.3 | 151 |

| # | Article | IF | CITATIONS |
|----|---|-----------------|------------------|
| 37 | Radiotheranostics: a roadmap for future development. Lancet Oncology, The, 2020, 21, e146-e156. | 10.7 | 151 |
| 38 | HER2-Mediated Internalization of Cytotoxic Agents in <i>ERBB2</i> Amplified or Mutant Lung Cancers. Cancer Discovery, 2020, 10, 674-687. | 9.4 | 149 |
| 39 | Detection of HER2-Positive Metastases in Patients with HER2-Negative Primary Breast Cancer Using ⁸⁹ Zr-Trastuzumab PET/CT. Journal of Nuclear Medicine, 2016, 57, 1523-1528. | 5.0 | 146 |
| 40 | PET Imaging of Tumor-Associated Macrophages with ⁸⁹ Zr-Labeled High-Density Lipoprotein Nanoparticles. Journal of Nuclear Medicine, 2015, 56, 1272-1277. | 5.0 | 145 |
| 41 | Magnitude of Enhanced Permeability and Retention Effect in Tumors with Different Phenotypes: ⁸⁹ Zr-Albumin as a Model System. Journal of Nuclear Medicine, 2011, 52, 625-633. | 5.0 | 144 |
| 42 | Alternative Chelator for ⁸⁹ Zr Radiopharmaceuticals: Radiolabeling and Evaluation of 3,4,3-(LI-1,2-HOPO). Journal of Medicinal Chemistry, 2014, 57, 4849-4860. | 6.4 | 143 |
| 43 | Modular Strategy for the Construction of Radiometalated Antibodies for Positron Emission Tomography Based on Inverse Electron Demand Diels–Alder Click Chemistry. Bioconjugate Chemistry, 2011, 22, 2048-2059. | 3.6 | 142 |
| 44 | High purity production and potential applications of copper-60 and copper-61. Nuclear Medicine and Biology, 1999, 26, 351-358. | 0.6 | 140 |
| 45 | Multiplexed imaging for diagnosis and therapy. Nature Biomedical Engineering, 2017, 1, 697-713. | 22.5 | 133 |
| 46 | Tumor uptake of copper-diacetyl-bis(N(4)-methylthiosemicarbazone): effect of changes in tissue oxygenation. Journal of Nuclear Medicine, 2001, 42, 655-61. | 5.0 | 133 |
| 47 | α-Emitters for Radiotherapy: From Basic Radiochemistry to Clinical Studies—Part 1. Journal of Nuclear Medicine, 2018, 59, 878-884. | 5.0 | 131 |
| 48 | 89Zr-huJ591 immuno-PET imaging in patients with advanced metastatic prostate cancer. European Journal of Nuclear Medicine and Molecular Imaging, 2014, 41, 2093-2105. | 6.4 | 130 |
| 49 | Medical imaging and nuclear medicine: a Lancet Oncology Commission. Lancet Oncology, The, 2021, 22, e136-e172. | 10.7 | 129 |
| 50 | ¹⁸ F-Based Pretargeted PET Imaging Based on Bioorthogonal Diels–Alder Click Chemistry. Bioconjugate Chemistry, 2016, 27, 298-301. | 3.6 | 127 |
| 51 | Retention mechanism of hypoxia selective nuclear imaging/radiotherapeutic agent Cu-diacetyl-bis(N) Tj ETQq1 1 C |).784314 2.2 | rgBT/Over 126 |
| 52 | Unconventional Nuclides for Radiopharmaceuticals. Molecular Imaging, 2010, 9, 7290.2010.00008. | 1.4 | 126 |
| 53 | First-in-Human Human Epidermal Growth Factor Receptor 2–Targeted Imaging Using ⁸⁹ Zr-Pertuzumab PET/CT: Dosimetry and Clinical Application in Patients with Breast Cancer. Journal of Nuclear Medicine, 2018, 59, 900-906. | 5.0 | 126 |
| 54 | Imaging of Melanoma Using64Cuâ^' and86Yâ^'DOTAâ^'ReCCMSH(Arg11), a Cyclized Peptide Analogue of α-MSH. Journal of Medicinal Chemistry, 2005, 48, 2985-2992. | 6.4 | 124 |

| # | Article | IF | CITATIONS |
|----|---|------|-----------|
| 55 | Enzyme-Mediated Methodology for the Site-Specific Radiolabeling of Antibodies Based on Catalyst-Free Click Chemistry. Bioconjugate Chemistry, 2013, 24, 1057-1067. | 3.6 | 123 |
| 56 | Antagonism of EGFR and HER3 Enhances the Response to Inhibitors of the PI3K-Akt Pathway in Triple-Negative Breast Cancer. Science Signaling, 2014, 7, ra29. | 3.6 | 123 |
| 57 | Measuring the Pharmacodynamic Effects of a Novel Hsp90 Inhibitor on HER2/neu Expression in Mice Using 89Zr-DFO-Trastuzumab. PLoS ONE, 2010, 5, e8859. | 2.5 | 121 |
| 58 | Imaging and treating tumor vasculature with targeted radiolabeled carbon nanotubes. International Journal of Nanomedicine, 2010, 5, 783. | 6.7 | 117 |
| 59 | ⁸⁹ Zr-Labeled Dextran Nanoparticles Allow in Vivo Macrophage Imaging. Bioconjugate Chemistry, 2011, 22, 2383-2389. | 3.6 | 116 |
| 60 | First-in-Human Imaging with ⁸⁹ Zr-Df-IAB2M Anti-PSMA Minibody in Patients with Metastatic Prostate Cancer: Pharmacokinetics, Biodistribution, Dosimetry, and Lesion Uptake. Journal of Nuclear Medicine, 2016, 57, 1858-1864. | 5.0 | 116 |
| 61 | <i>EGFR</i> and <i>MET</i> Amplifications Determine Response to HER2 Inhibition in <i>ERBB2</i> -Amplified Esophagogastric Cancer. Cancer Discovery, 2019, 9, 199-209. | 9.4 | 115 |
| 62 | Preparation of 66Ga- and 68Ga-labeled Ga(III)-deferoxamine-folate as potential folate-receptor-targeted PET radiopharmaceuticals. Nuclear Medicine and Biology, 2003, 30, 725-731. | 0.6 | 113 |
| 63 | The Growing Impact of Bioorthogonal Click Chemistry on the Development of Radiopharmaceuticals. Journal of Nuclear Medicine, 2013, 54, 829-832. | 5.0 | 108 |
| 64 | Measurement of input functions in rodents: challenges and solutions. Nuclear Medicine and Biology, 2005, 32, 679-685. | 0.6 | 107 |
| 65 | Androgen Receptor Upregulation Mediates Radioresistance after Ionizing Radiation. Cancer Research, 2015, 75, 4688-4696. | 0.9 | 105 |
| 66 | <i>p</i> -SCN-Bn-HOPO: A Superior Bifunctional Chelator for ⁸⁹ Zr ImmunoPET. Bioconjugate Chemistry, 2015, 26, 2579-2591. | 3.6 | 104 |
| 67 | Comparison of Four64Cu-Labeled Somatostatin Analogues in Vitro and in a Tumor-Bearing Rat Model:Â Evaluation of New Derivatives for Positron Emission Tomography Imaging and Targeted Radiotherapy‖. Journal of Medicinal Chemistry, 1999, 42, 1341-1347. | 6.4 | 99 |
| 68 | Cell line-dependent differences in uptake and retention of the hypoxia-selective nuclear imaging agent Cu-ATSM. Nuclear Medicine and Biology, 2005, 32, 623-630. | 0.6 | 98 |
| 69 | Pharmacokinetics, Biodistribution, and Radiation Dosimetry for ⁸⁹ Zr-Trastuzumab in Patients with Esophagogastric Cancer. Journal of Nuclear Medicine, 2018, 59, 161-166. | 5.0 | 96 |
| 70 | Biodistribution and Dosimetry of ¹⁸ F-Meta-Fluorobenzylguanidine: A First-in-Human PET/CT Imaging Study of Patients with Neuroendocrine Malignancies. Journal of Nuclear Medicine, 2018, 59, 147-153. | 5.0 | 96 |
| 71 | Design of hypoxia-targeting radiopharmaceuticals: selective uptake of copper-64 complexes in hypoxic cells in vitro. European Journal of Nuclear Medicine and Molecular Imaging, 1998, 25, 788-792. | 6.4 | 94 |
| 72 | Nanoreporter PET predicts the efficacy of anti-cancer nanotherapy. Nature Communications, 2016, 7, 11838. | 12.8 | 94 |

| # | Article | IF | CITATIONS |
|----|--|------|-----------|
| 73 | Basic characterization of 64Cu-ATSM as a radiotherapy agent. Nuclear Medicine and Biology, 2005, 32, 21-28. | 0.6 | 93 |
| 74 | The Next Generation of Positron Emission Tomography Radiopharmaceuticals in Oncology. Seminars in Nuclear Medicine, 2011, 41, 265-282. | 4.6 | 93 |
| 75 | Positron Emission Tomography/Computed Tomography–Based Assessments of Androgen Receptor Expression and Glycolytic Activity as a Prognostic Biomarker for Metastatic Castration-Resistant Prostate Cancer. JAMA Oncology, 2018, 4, 217. | 7.1 | 93 |
| 76 | Tim-4+ cavity-resident macrophages impair anti-tumor CD8+ TÂcell immunity. Cancer Cell, 2021, 39, 973-988.e9. | 16.8 | 93 |
| 77 | Radiopharmaceuticals in Preclinical and Clinical Development for Monitoring of Therapy with PET. Journal of Nuclear Medicine, 2009, 50, 106S-121S. | 5.0 | 92 |
| 78 | Radiotheranostics in oncology: current challenges and emerging opportunities. Nature Reviews Clinical Oncology, 2022, 19, 534-550. | 27.6 | 92 |
| 79 | Noninvasive Interrogation of DLL3 Expression in Metastatic Small Cell Lung Cancer. Cancer Research, 2017, 77, 3931-3941. | 0.9 | 91 |
| 80 | Applications of pHLIP Technology for Cancer Imaging and Therapy. Trends in Biotechnology, 2017, 35, 653-664. | 9.3 | 90 |
| 81 | In vitro and in vivo evaluation of 64Cu-TETA-Tyr3-octreotate. a new somatostatin analog with improved target tissue uptake. Nuclear Medicine and Biology, 1999, 26, 267-273. | 0.6 | 88 |
| 82 | Fatty Acid Synthase Is a Key Target in Multiple Essential Tumor Functions of Prostate Cancer: Uptake of Radiolabeled Acetate as a Predictor of the Targeted Therapy Outcome. PLoS ONE, 2013, 8, e64570. | 2.5 | 88 |
| 83 | Optimization of a Pretargeted Strategy for the PET Imaging of Colorectal Carcinoma via the Modulation of Radioligand Pharmacokinetics. Molecular Pharmaceutics, 2015, 12, 3575-3587. | 4.6 | 88 |
| 84 | 64Cu-Labeled CB-TE2A and diamsar-conjugated RGD peptide analogs for targeting angiogenesis: comparison of their biological activity. Nuclear Medicine and Biology, 2009, 36, 277-285. | 0.6 | 87 |
| 85 | Monitoring Afatinib Treatment in HER2-Positive Gastric Cancer with 18F-FDG and 89Zr-Trastuzumab PET. Journal of Nuclear Medicine, 2013, 54, 936-943. | 5.0 | 85 |
| 86 | A Modular Labeling Strategy for In Vivo PET and Near-Infrared Fluorescence Imaging of Nanoparticle Tumor Targeting. Journal of Nuclear Medicine, 2014, 55, 1706-1711. | 5.0 | 85 |
| 87 | Site-specifically labeled CA19.9-targeted immunoconjugates for the PET, NIRF, and multimodal PET/NIRF imaging of pancreatic cancer. Proceedings of the National Academy of Sciences of the United States of America, 2015, 112, 15850-15855. | 7.1 | 85 |
| 88 | Radiotherapy, toxicity and dosimetry of copper-64-TETA-octreotide in tumor-bearing rats. Journal of Nuclear Medicine, 1998, 39, 1944-51. | 5.0 | 85 |
| 89 | Annotating MYC status with 89Zr-transferrin imaging. Nature Medicine, 2012, 18, 1586-1591. | 30.7 | 83 |
| 90 | Autoradiographic and small-animal PET comparisons between 18F-FMISO, 18F-FDG, 18F-FLT and the hypoxic selective 64Cu-ATSM in a rodent model of cancer. Nuclear Medicine and Biology, 2008, 35, 713-720. | 0.6 | 82 |

| # | Article | IF | CITATIONS |
|-----|---|------|-----------|
| 91 | H ₄ octapa-Trastuzumab: Versatile Acyclic Chelate System for ¹¹¹ In and ¹⁷⁷ Lu Imaging and Therapy. Journal of the American Chemical Society, 2013, 135, 12707-12721. | 13.7 | 82 |
| 92 | Preparation of high specific activity 86Y using a small biomedical cyclotron. Nuclear Medicine and Biology, 2005, 32, 891-897. | 0.6 | 81 |
| 93 | 89Zr-Labeled Paramagnetic Octreotide-Liposomes for PET-MR Imaging of Cancer. Pharmaceutical Research, 2013, 30, 878-888. | 3.5 | 81 |
| 94 | Distant metastasis in p16-positive oropharyngeal squamous cell carcinoma: A critical analysis of patterns and outcomes. Oral Oncology, 2014, 50, 45-51. | 1.5 | 81 |
| 95 | 89Zr-Trastuzumab PET/CT for Detection of Human Epidermal Growth Factor Receptor 2–Positive Metastases in Patients With Human Epidermal Growth Factor Receptor 2–Negative Primary Breast Cancer. Clinical Nuclear Medicine, 2017, 42, 912-917. | 1.3 | 81 |
| 96 | Pretargeted Immuno-PET of Pancreatic Cancer: Overcoming Circulating Antigen and Internalized Antibody to Reduce Radiation Doses. Journal of Nuclear Medicine, 2016, 57, 453-459. | 5.0 | 80 |
| 97 | In Vivo PET Assay of Tumor Glutamine Flux and Metabolism: In-Human Trial of ¹⁸ F-(2 <i>S</i> ,4 <i>R</i>)-4-Fluoroglutamine. Radiology, 2018, 287, 667-675. | 7.3 | 80 |
| 98 | Establishment of the <i>In Vivo</i> Efficacy of Pretargeted Radioimmunotherapy Utilizing Inverse Electron Demand Diels-Alder Click Chemistry. Molecular Cancer Therapeutics, 2017, 16, 124-133. | 4.1 | 79 |
| 99 | InÂVivo PET Imaging of HDL in MultipleÂAtherosclerosisÂModels. JACC: Cardiovascular Imaging, 2016, 9, 950-961. | 5.3 | 78 |
| 100 | Caveolin-1 mediates cellular distribution of HER2 and affects trastuzumab binding and therapeutic efficacy. Nature Communications, 2018, 9, 5137. | 12.8 | 78 |
| 101 | In Vivo Biodistribution, PET Imaging, and Tumor Accumulation of ⁸⁶ Y- and ¹¹¹ In-Antimindin/RG-1, Engineered Antibody Fragments in LNCaP Tumor–Bearing Nude Mice. Journal of Nuclear Medicine, 2009, 50, 435-443. | 5.0 | 76 |
| 102 | Underscoring the Influence of Inorganic Chemistry on Nuclear Imaging with Radiometals. Inorganic Chemistry, 2014, 53, 1880-1899. | 4.0 | 75 |
| 103 | Dosimetry of 60/61/62/64Cu-ATSM: a hypoxia imaging agent for PET. European Journal of Nuclear Medicine and Molecular Imaging, 2005, 32, 764-770. | 6.4 | 74 |
| 104 | ¹⁸ F-Labeled-Bioorthogonal Liposomes for <i>In Vivo</i> Targeting. Bioconjugate Chemistry, 2013, 24, 1784-1789. | 3.6 | 74 |
| 105 | A Prospective Pilot Study of ⁸⁹ Zr-J591/Prostate Specific Membrane Antigen Positron Emission Tomography in Men with Localized Prostate Cancer Undergoing Radical Prostatectomy. Journal of Urology, 2014, 191, 1439-1445. | 0.4 | 73 |
| 106 | CD38-targeted Immuno-PET of Multiple Myeloma: From Xenograft Models to First-in-Human Imaging. Radiology, 2020, 295, 606-615. | 7.3 | 73 |
| 107 | In Vitro and In Vivo Evaluation of Bifunctional Bisthiosemicarbazone ⁶⁴ Cu-Complexes for the Positron Emission Tomography Imaging of Hypoxia. Journal of Medicinal Chemistry, 2008, 51, 2985-2991. | 6.4 | 72 |
| 108 | α-Emitters for Radiotherapy: From Basic Radiochemistry to Clinical Studies—Part 2. Journal of Nuclear Medicine, 2018, 59, 1020-1027. | 5.0 | 72 |

| # | Article | IF | CITATIONS |
|-----|--|------|-----------|
| 109 | Radiotherapy and dosimetry of 64Cu-TETA-Tyr3-octreotate in a somatostatin receptor-positive, tumor-bearing rat model. Clinical Cancer Research, 1999, 5, 3608-16. | 7.0 | 71 |
| 110 | DOTAâ | 3.6 | 69 |
| 111 | Fc-Mediated Anomalous Biodistribution of Therapeutic Antibodies in Immunodeficient Mouse Models. Cancer Research, 2018, 78, 1820-1832. | 0.9 | 69 |
| 112 | Phase I Trial of Well-Differentiated Neuroendocrine Tumors (NETs) with Radiolabeled Somatostatin Antagonist 177Lu-Satoreotide Tetraxetan. Clinical Cancer Research, 2019, 25, 6939-6947. | 7.0 | 69 |
| 113 | Targeted Brain Tumor Radiotherapy Using an Auger Emitter. Clinical Cancer Research, 2020, 26, 2871-2881. | 7.0 | 69 |
| 114 | Head-to-Head Evaluation of ¹⁸ F-FES and ¹⁸ F-FDG PET/CT in Metastatic Invasive Lobular Breast Cancer. Journal of Nuclear Medicine, 2021, 62, 326-331. | 5.0 | 69 |
| 115 | Delineation of hypoxia in canine myocardium using PET and copper(II)-diacetyl-bis(N(4)-methylthiosemicarbazone). Journal of Nuclear Medicine, 2002, 43, 1557-69. | 5.0 | 69 |
| 116 | Investigation into 64Cu-labeled Bis(selenosemicarbazone) and Bis(thiosemicarbazone) complexes as hypoxia imaging agents. Nuclear Medicine and Biology, 2005, 32, 147-156. | 0.6 | 68 |
| 117 | Imaging Androgen Receptor Signaling with a Radiotracer Targeting Free Prostate-Specific Antigen. Cancer Discovery, 2012, 2, 320-327. | 9.4 | 68 |
| 118 | Development of a minimal saponin vaccine adjuvant based on QS-21. Nature Chemistry, 2014, 6, 635-643. | 13.6 | 68 |
| 119 | Harnessing ⁶⁴ Cu/ ⁶⁷ Cu for a theranostic approach to pretargeted radioimmunotherapy. Proceedings of the National Academy of Sciences of the United States of America, 2020, 117, 28316-28327. | 7.1 | 67 |
| 120 | The Future of Nuclear Medicine, Molecular Imaging, and Theranostics. Journal of Nuclear Medicine, 2020, 61, 263S-272S. | 5.0 | 67 |
| 121 | Nanobody-Facilitated Multiparametric PET/MRI Phenotyping of Atherosclerosis. JACC: Cardiovascular Imaging, 2019, 12, 2015-2026. | 5.3 | 66 |
| 122 | Positron-Emitting Isotopes Produced on Biomedical Cyclotrons. Current Medicinal Chemistry, 2005, 12, 807-818. | 2.4 | 65 |
| 123 | Molecular Imaging of Gastrin-Releasing Peptide Receptor-Positive Tumors in Mice Using ⁶⁴ Cu- and ⁸⁶ Y-DOTAâ^'(Pro ¹ ,Tyr ⁴)-Bombesin(1â^'14). Bioconjugate Chemistry, 2007, 18, 724-730. | 3.6 | 65 |
| 124 | Noninvasive Imaging of PSMA in Prostate Tumors with ⁸⁹ Zr-Labeled huJ591 Engineered Antibody Fragments: The Faster Alternatives. Molecular Pharmaceutics, 2014, 11, 3965-3973. | 4.6 | 65 |
| 125 | Pairwise comparison of 89Zr- and 124I-labeled cG250 based on positron emission tomography imaging and nonlinear immunokinetic modeling: in vivo carbonic anhydrase IX receptor binding and internalization in mouse xenografts of clear-cell renal cell carcinoma. European Journal of Nuclear Medicine and Molecular Imaging, 2014, 41, 985-994. | 6.4 | 65 |
| 126 | NuMA Influences Higher Order Chromatin Organization in Human Mammary Epithelium. Molecular Biology of the Cell, 2007, 18, 348-361. | 2.1 | 64 |

| # | Article | IF | CITATIONS |
|-----|--|------|-----------|
| 127 | Feasibility and Predictability of Perioperative PET and Estrogen Receptor Ligand in Patients with Invasive Breast Cancer. Journal of Nuclear Medicine, 2013, 54, 1697-1702. | 5.0 | 64 |
| 128 | Chemoenzymatic Strategy for the Synthesis of Site-Specifically Labeled Immunoconjugates for Multimodal PET and Optical Imaging. Bioconjugate Chemistry, 2014, 25, 2123-2128. | 3.6 | 64 |
| 129 | Delivery of polymeric nanostars for molecular imaging and endoradiotherapy through the enhanced permeability and retention (EPR) effect. Theranostics, 2020, 10, 567-584. | 10.0 | 63 |
| 130 | Imaging the Norepinephrine Transporter in Neuroblastoma: A Comparison of [18F]-MFBG and 123I-MIBG. Clinical Cancer Research, 2014, 20, 2182-2191. | 7.0 | 61 |
| 131 | Efficient ¹⁸ F-Labeling of Large 37-Amino-Acid pHLIP Peptide Analogues and Their Biological Evaluation. Bioconjugate Chemistry, 2012, 23, 1557-1566. | 3.6 | 60 |
| 132 | Pretargeted PET Imaging Using a Site-Specifically Labeled Immunoconjugate. Bioconjugate Chemistry, 2016, 27, 1789-1795. | 3.6 | 60 |
| 133 | Initial Results of a Prospective Clinical Trial of ¹⁸ F-Fluciclovine PET/CT in Newly Diagnosed Invasive Ductal and Invasive Lobular Breast Cancers. Journal of Nuclear Medicine, 2016, 57, 1350-1356. | 5.0 | 60 |
| 134 | The Bioconjugation and Radiosynthesis of ⁸⁹ Zr-DFO-labeled Antibodies. Journal of Visualized Experiments, 2015, , . | 0.3 | 60 |
| 135 | Applying PET to Broaden the Diagnostic Utility of the Clinically Validated CA19.9 Serum Biomarker for Oncology. Journal of Nuclear Medicine, 2013, 54, 1876-1882. | 5.0 | 58 |
| 136 | Pretargeting of internalizing trastuzumab and cetuximab with a 18F-tetrazine tracer in xenograft models. EJNMMI Research, 2017, 7, 95. | 2.5 | 58 |
| 137 | Intraoperative imaging of positron emission tomographic radiotracers using Cerenkov luminescence emissions. Molecular Imaging, 2011, 10, 177-86, 1-3. | 1.4 | 58 |
| 138 | H6phospa-trastuzumab: bifunctional methylenephosphonate-based chelator with89Zr,111In and177Lu. Dalton Transactions, 2014, 43, 119-131. | 3.3 | 57 |
| 139 | Targeting Breast Tumors with pH (Low) Insertion Peptides. Molecular Pharmaceutics, 2014, 11, 2896-2905. | 4.6 | 57 |
| 140 | Synthesis and biologic evaluation of 64Cu-labeled rhenium-cyclized alpha-MSH peptide analog using a cross-bridged cyclam chelator. Journal of Nuclear Medicine, 2007, 48, 64-72. | 5.0 | 57 |
| 141 | Targeting the Internal Epitope of Prostate-Specific Membrane Antigen with ⁸⁹ Zr-7E11 Immuno-PET. Journal of Nuclear Medicine, 2011, 52, 1608-1615. | 5.0 | 56 |
| 142 | Assessing tumor hypoxia by positron emission tomography with Cu-ATSM. Quarterly Journal of Nuclear Medicine and Molecular Imaging, 2009, 53, 193-200. | 0.7 | 56 |
| 143 | Intra-tumoral distribution of 64Cu-ATSM: a comparison study with FDG. Nuclear Medicine and Biology, 2003, 30, 529-534. | 0.6 | 55 |
| 144 | Leveraging Bioorthogonal Click Chemistry to Improve 225Ac-Radioimmunotherapy of Pancreatic Ductal Adenocarcinoma. Clinical Cancer Research, 2019, 25, 868-880. | 7.0 | 55 |

| # | Article | IF | CITATIONS |
|-----|--|------|-----------|
| 145 | Melanoma imaging using 111In-, 86Y- and 68Ga-labeled CHX-A″-Re(Arg11)CCMSH. Nuclear Medicine and Biology, 2009, 36, 345-354. | 0.6 | 53 |
| 146 | Intraoperative Imaging of Positron Emission Tomographic Radiotracers Using Cerenkov Luminescence Emissions. Molecular Imaging, 2011, 10, 7290.2010.00047. | 1.4 | 53 |
| 147 | A Pretargeted Approach for the Multimodal PET/NIRF Imaging of Colorectal Cancer. Theranostics, 2016, 6, 2267-2277. | 10.0 | 53 |
| 148 | H ₂ azapa: a Versatile Acyclic Multifunctional Chelator for ⁶⁷ Ga, ⁶⁴ Cu, ¹¹¹ In, and ¹⁷⁷ Lu. Inorganic Chemistry, 2012, 51, 12575-12589. | 4.0 | 52 |
| 149 | PET Imaging of Extracellular pH in Tumors with ⁶⁴ Cu- and ¹⁸ F-Labeled pHLIP Peptides: A Structure–Activity Optimization Study. Bioconjugate Chemistry, 2016, 27, 2014-2023. | 3.6 | 52 |
| 150 | Exploring Structural Parameters for Pretargeting Radioligand Optimization. Journal of Medicinal Chemistry, 2017, 60, 8201-8217. | 6.4 | 52 |
| 151 | Unconventional nuclides for radiopharmaceuticals. Molecular Imaging, 2010, 9, 1-20. | 1.4 | 52 |
| 152 | Toxicity and dosimetry of177Lu-DOTA-Y3-octreotate in a rat model. International Journal of Cancer, 2001, 94, 873-877. | 5.1 | 51 |
| 153 | Examining the relationship between Cu-ATSM hypoxia selectivity and fatty acid synthase expression in human prostate cancer cell lines. Nuclear Medicine and Biology, 2008, 35, 273-279. | 0.6 | 51 |
| 154 | PARP-1–Targeted Radiotherapy in Mouse Models of Glioblastoma. Journal of Nuclear Medicine, 2018, 59, 1225-1233. | 5.0 | 51 |
| 155 | Nitroimidazole conjugates of bis(thiosemicarbazonato)64Cu(II) – Potential combination agents for the PET imaging of hypoxia. Journal of Inorganic Biochemistry, 2010, 104, 126-135. | 3.5 | 50 |
| 156 | Synthesis and evaluation of 18F-labeled benzylguanidine analogs for targeting the human norepinephrine transporter. European Journal of Nuclear Medicine and Molecular Imaging, 2014, 41, 322-332. | 6.4 | 50 |
| 157 | The Impact of Positron Range on PET Resolution, Evaluated with Phantoms and PHITS Monte Carlo Simulations for Conventional and Non-conventional Radionuclides. Molecular Imaging and Biology, 2020, 22, 73-84. | 2.6 | 50 |
| 158 | Human Epidermal Growth Factor Receptor 2-Targeted PET/Single- Photon Emission Computed Tomography Imaging of Breast Cancer. PET Clinics, 2017, 12, 269-288. | 3.0 | 49 |
| 159 | Validation of a Novel CHX-Aâ€ [~] Ââ€ [~] Derivative Suitable for Peptide Conjugation: Small Animal PET/CT Imaging Using Yttrium-86-CHX-Aâ€ [~] Ââ€ [~] -Octreotide. Journal of Medicinal Chemistry, 2006, 49, 4297-4304. | 6.4 | 48 |
| 160 | Gallium-68-labeled DOTA-rhenium-cyclized α-melanocyte-stimulating hormone analog for imaging of malignant melanoma. Nuclear Medicine and Biology, 2007, 34, 945-953. | 0.6 | 47 |
| 161 | Prospective Clinical Trial of ¹⁸ F-Fluciclovine PET/CT for Determining the Response to Neoadjuvant Therapy in Invasive Ductal and Invasive Lobular Breast Cancers. Journal of Nuclear Medicine, 2017, 58, 1037-1042. | 5.0 | 47 |
| 162 | Retooling a Blood-Based Biomarker: Phase I Assessment of the High-Affinity CA19-9 Antibody HuMab-5B1 for Immuno-PET Imaging of Pancreatic Cancer. Clinical Cancer Research, 2019, 25, 7014-7023. | 7.0 | 47 |

| # | Article | IF | CITATIONS |
|-----|---|------|-----------|
| 163 | In vivo skeletal imaging of 18F-fluoride with positron emission tomography reveals damage- and time-dependent responses to fatigue loading in the rat ulna. Bone, 2006, 39, 229-236. | 2.9 | 46 |
| 164 | Synthesis, in vitro and in vivo characterization of 64Cu(I) complexes derived from hydrophilic tris(hydroxymethyl)phosphane and 1,3,5-triaza-7-phosphaadamantane ligands. Journal of Biological Inorganic Chemistry, 2008, 13, 307-315. | 2.6 | 46 |
| 165 | A phase II study of radioimmunotherapy with intraventricular ¹³¹ lâ€3F8 for medulloblastoma. Pediatric Blood and Cancer, 2018, 65, e26754. | 1.5 | 46 |
| 166 | Enhancing targeted radiotherapy by copper(II)diacetyl- bis(N4-methylthiosemicarbazone) using 2-deoxy-D-glucose. Cancer Research, 2003, 63, 5496-504. | 0.9 | 46 |
| 167 | Identification of a Novel Prostate Tumor Target, Mindin/RG-1, for Antibody-Based Radiotherapy of Prostate Cancer. Cancer Research, 2005, 65, 8397-8405. | 0.9 | 44 |
| 168 | Intraoperative Imaging of Positron Emission Tomographic Radiotracers Using Cerenkov Luminescence Emissions. Molecular Imaging, 2011, 10, 7290.2010.00047. | 1.4 | 44 |
| 169 | Challenges of Pancreatic Cancer. Cancer Journal (Sudbury, Mass), 2015, 21, 188-193. | 2.0 | 44 |
| 170 | Biodistribution and radiation dose estimates for 68Ga-DOTA-JR11 in patients with metastatic neuroendocrine tumors. European Journal of Nuclear Medicine and Molecular Imaging, 2019, 46, 677-685. | 6.4 | 44 |
| 171 | Recent Advances in Radiometals for Combined Imaging and Therapy in Cancer. ChemMedChem, 2021, 16, 2909-2941. | 3.2 | 44 |
| 172 | Clickable bifunctional radiometal chelates for peptide labeling. Chemical Communications, 2010, 46, 1706. | 4.1 | 43 |
| 173 | Copper bis(diphosphine) complexes: radiopharmaceuticals for the detection of multi-drug resistance in tumours by PET. European Journal of Nuclear Medicine and Molecular Imaging, 2000, 27, 638-646. | 6.4 | 40 |
| 174 | Understanding the pharmacological properties of a metabolic PET tracer in prostate cancer. Proceedings of the National Academy of Sciences of the United States of America, 2014, 111, 7254-7259. | 7.1 | 40 |
| 175 | Paradigms for Precision Medicine in Epichaperome Cancer Therapy. Cancer Cell, 2019, 36, 559-573.e7. | 16.8 | 40 |
| 176 | B7H3-Directed Intraperitoneal Radioimmunotherapy With Radioiodinated Omburtamab for Desmoplastic Small Round Cell Tumor and Other Peritoneal Tumors: Results of a Phase I Study. Journal of Clinical Oncology, 2020, 38, 4283-4291. | 1.6 | 40 |
| 177 | Identification of HER2-Positive Metastases in Patients with HER2-Negative Primary Breast Cancer by Using HER2-targeted ⁸⁹ Zr-Pertuzumab PET/CT. Radiology, 2020, 296, 370-378. | 7.3 | 40 |
| 178 | What a Difference a Carbon Makes: H ₄ octapa vs H ₄ C3octapa, Ligands for In-111 and Lu-177 Radiochemistry. Inorganic Chemistry, 2014, 53, 10412-10431. | 4.0 | 38 |
| 179 | IN VIVO IMAGING IN A MURINE MODEL OF GLIOBLASTOMA. Neurosurgery, 2007, 60, 360-371. | 1.1 | 37 |
| 180 | Feed-forward alpha particle radiotherapy ablates androgen receptor-addicted prostate cancer. Nature Communications, 2018, 9, 1629. | 12.8 | 37 |

| # | Article | IF | CITATIONS |
|-----|--|------|-----------|
| 181 | Click-Mediated Pretargeted Radioimmunotherapy of Colorectal Carcinoma. Molecular Pharmaceutics, 2018, 15, 1729-1734. | 4.6 | 36 |
| 182 | Safety and Feasibility of PARP1/2 Imaging with 18F-PARPi in Patients with Head and Neck Cancer. Clinical Cancer Research, 2020, 26, 3110-3116. | 7.0 | 36 |
| 183 | Three-dimensional maximum a posteriori (MAP) imaging with radiopharmaceuticals labeled with three Cu radionuclides. Nuclear Medicine and Biology, 2006, 33, 217-226. | 0.6 | 35 |
| 184 | Bioorthogonal Masking of Circulating Antibody–TCO Groups Using Tetrazine-Functionalized Dextran Polymers. Bioconjugate Chemistry, 2018, 29, 538-545. | 3.6 | 35 |
| 185 | Evaluation of Hypoxia With Copper-Labeled Diacetyl-bis(N-Methylthiosemicarbazone). Seminars in Nuclear Medicine, 2015, 45, 177-185. | 4.6 | 34 |
| 186 | A rapid bead-based radioligand binding assay for the determination of target-binding fraction and quality control of radiopharmaceuticals. Nuclear Medicine and Biology, 2019, 71, 32-38. | 0.6 | 34 |
| 187 | Molecular imaging: The application of small animal positron emission tomography. Journal of Cellular Biochemistry, 2002, 87, 110-115. | 2.6 | 33 |
| 188 | Imaging Tumor Burden in the Brain with ⁸⁹ Zr-Transferrin. Journal of Nuclear Medicine, 2013, 54, 90-95. | 5.0 | 33 |
| 189 | ⁸⁹ Zr-DFO-AMG102 Immuno-PET to Determine Local Hepatocyte Growth Factor Protein Levels in Tumors for Enhanced Patient Selection. Journal of Nuclear Medicine, 2017, 58, 1386-1394. | 5.0 | 33 |
| 190 | The inverse electron-demand Diels–Alder reaction as a new methodology for the synthesis of225Ac-labelled radioimmunoconjugates. Chemical Communications, 2018, 54, 2599-2602. | 4.1 | 33 |
| 191 | Improved synthesis of 2′-deoxy-2′-[18F]-fluoro-1-β-d-arabinofuranosyl-5-iodouracil ([18F]-FIAU). Nuclear Medicine and Biology, 2010, 37, 439-442. | 0.6 | 32 |
| 192 | Antibodies Against Specific MUC16 Glycosylation Sites Inhibit Ovarian Cancer Growth. ACS Chemical Biology, 2017, 12, 2085-2096. | 3.4 | 32 |
| 193 | Preclinical ⁸⁹ Zr Immuno-PET of High-Grade Serous Ovarian Cancer and Lymph Node Metastasis. Journal of Nuclear Medicine, 2016, 57, 771-776. | 5.0 | 31 |
| 194 | Preloading with Unlabeled CA19.9 Targeted Human Monoclonal Antibody Leads to Improved PET Imaging with ⁸⁹ Zr-5B1. Molecular Pharmaceutics, 2017, 14, 908-915. | 4.6 | 31 |
| 195 | Noninvasive Measurement of mTORC1 Signaling with 89Zr-Transferrin. Clinical Cancer Research, 2017, 23, 3045-3052. | 7.0 | 31 |
| 196 | Noninvasive ⁸⁹ Zr-Transferrin PET Shows Improved Tumor Targeting Compared with ¹⁸ F-FDG PET in MYC-Overexpressing Human Triple-Negative Breast Cancer. Journal of Nuclear Medicine, 2018, 59, 51-57. | 5.0 | 31 |
| 197 | The Influence of Glycans-Specific Bioconjugation on the Fcl̂ ³ RI Binding and <i>In vivo</i> Performance of ⁸⁹ Zr-DFO-Pertuzumab. Theranostics, 2020, 10, 1746-1757. | 10.0 | 31 |
| 198 | iNOS Regulates the Therapeutic Response of Pancreatic Cancer Cells to Radiotherapy. Cancer Research, 2020, 80, 1681-1692. | 0.9 | 31 |

| # | Article | IF | CITATIONS |
|-----|---|-----|-----------|
| 199 | Copper(I) bis(diphosphine) complexes as a basis for radiopharmaceuticals for positron emission tomography and targeted radiotherapy. Chemical Communications, 1996, , 1093. | 4.1 | 30 |
| 200 | Biodistribution and Dosimetry of Intraventricularly Administered ¹²⁴ I-Omburtamab in Patients with Metastatic Leptomeningeal Tumors. Journal of Nuclear Medicine, 2019, 60, 1794-1801. | 5.0 | 29 |
| 201 | Targeted PET imaging strategy to differentiate malignant from inflamed lymph nodes in diffuse large B-cell lymphoma. Proceedings of the National Academy of Sciences of the United States of America, 2017, 114, E7441-E7449. | 7.1 | 28 |
| 202 | A Tat Fusion Protein–Based Tumor Vaccine for Breast Cancer. Annals of Surgical Oncology, 2005, 12, 517-525. | 1.5 | 27 |
| 203 | An Anatomical Study of Tibial Metaphyseal/Diaphyseal Mismatch During Revision Total Knee Arthroplasty. Journal of Arthroplasty, 2007, 22, 241-244. | 3.1 | 27 |
| 204 | Diagnostic and prognostic value of ambulatory ECG (Holter) monitoring in patients with coronary heart disease: a review. Journal of Thrombosis and Thrombolysis, 2007, 23, 135-145. | 2.1 | 27 |
| 205 | Temporal Modulation of HER2 Membrane Availability Increases Pertuzumab Uptake and Pretargeted Molecular Imaging of Gastric Tumors. Journal of Nuclear Medicine, 2019, 60, 1569-1578. | 5.0 | 27 |
| 206 | PARaDIM: A PHITS-Based Monte Carlo Tool for Internal Dosimetry with Tetrahedral Mesh Computational Phantoms. Journal of Nuclear Medicine, 2019, 60, 1802-1811. | 5.0 | 27 |
| 207 | Imaging of human epidermal growth factor receptors for patient selection and response monitoring – From PET imaging and beyond. Cancer Letters, 2018, 419, 139-151. | 7.2 | 26 |
| 208 | A Systematic Evaluation of Antibody Modification and ⁸⁹ Zr-Radiolabeling for Optimized Immuno-PET. Bioconjugate Chemistry, 2021, 32, 1177-1191. | 3.6 | 26 |
| 209 | A simple strategy to reduce the salivary gland and kidney uptake of PSMA-targeting small molecule radiopharmaceuticals. European Journal of Nuclear Medicine and Molecular Imaging, 2021, 48, 2642-2651. | 6.4 | 26 |
| 210 | Copper-64-pyruvaldehyde-bis(N(4)-methylthiosemicarbazone) for the prevention of tumor growth at wound sites following laparoscopic surgery: monitoring therapy response with microPET and magnetic resonance imaging. Cancer Research, 2002, 62, 445-9. | 0.9 | 26 |
| 211 | Annotating STEAP1 Regulation in Prostate Cancer with 89Zr Immuno-PET. Journal of Nuclear Medicine, 2014, 55, 2045-2049. | 5.0 | 25 |
| 212 | A comparative evaluation of the chelators H 4 octapa and CHX-A″-DTPA with the therapeutic radiometal 90 Y. Nuclear Medicine and Biology, 2016, 43, 566-576. | 0.6 | 25 |
| 213 | An ⁸⁹ Zr-HDL PET Tracer Monitors Response to a CSF1R Inhibitor. Journal of Nuclear Medicine, 2020, 61, 433-436. | 5.0 | 25 |
| 214 | Comparative Dosimetry of Copper-64 and Yttrium-90-Labeled Somatostatin Analogs in a Tumor-Bearing Rat Model. Cancer Biotherapy and Radiopharmaceuticals, 2000, 15, 593-604. | 1.0 | 24 |
| 215 | Building Blocks for the Construction of Bioorthogonally Reactive Peptides via Solidâ€Phase Peptide Synthesis. ChemistryOpen, 2014, 3, 48-53. | 1.9 | 24 |
| 216 | Preclinical optimization of antibodyâ€based radiopharmaceuticals for cancer imaging and radionuclide therapy—Model, vector, and radionuclide selection. Journal of Labelled Compounds and Radiopharmaceuticals, 2018, 61, 611-635. | 1.0 | 24 |

| # | ARTICLE | IF | CITATIONS |
|-----|---|---------------------|---------------|
| 217 | Trastuzumab gold-conjugates: synthetic approach and <i>in vitro</i> evaluation of anticancer activities in breast cancer cell lines. Chemical Communications, 2019, 55, 1394-1397. | 4.1 | 24 |
| 218 | Internalization of secreted antigen–targeted antibodies by the neonatal Fc receptor for precision imaging of the androgen receptor axis. Science Translational Medicine, 2016, 8, 367ra167. | 12.4 | 23 |
| 219 | ImmunoPET Predicts Response to Met-targeted Radioligand Therapy in Models of Pancreatic Cancer Resistant to Met Kinase Inhibitors. Theranostics, 2020, 10, 151-165. | 10.0 | 23 |
| 220 | Effect of ligand and solvent on chloride ion coordination in anti-tumour copper(I) diphosphine complexes: Synthesis of [Cu(dppe)2]Cl and analogous complexes (dppe =) Tj ETQq0 0 0 rgBT /Overlock 10 Tf 50 (| 6 ⊉7 2⊤d (1, | 2929is(dipher |
| 221 | Low incidence of radionecrosis in children treated with conventional radiation therapy and intrathecal radioimmunotherapy. Journal of Neuro-Oncology, 2015, 123, 245-249. | 2.9 | 22 |
| 222 | Current status and future challenges for molecular imaging. Philosophical Transactions Series A, Mathematical, Physical, and Engineering Sciences, 2017, 375, 20170023. | 3.4 | 22 |
| 223 | Tumor-Specific Zr-89 Immuno-PET Imaging in a Human Bladder Cancer Model. Molecular Imaging and Biology, 2018, 20, 808-815. | 2.6 | 22 |
| 224 | Multimodal Positron Emission Tomography Imaging to Quantify Uptake of ⁸⁹ Zr-Labeled Liposomes in the Atherosclerotic Vessel Wall. Bioconjugate Chemistry, 2020, 31, 360-368. | 3.6 | 22 |
| 225 | 64Cu-azabicyclo[3.2.2]nonane thiosemicarbazone complexes: radiopharmaceuticals for PET of topoisomerase II expression in tumors. Journal of Nuclear Medicine, 2006, 47, 2034-41. | 5.0 | 22 |
| 226 | Selective Imaging of VEGFR-1 and VEGFR-2 Using ⁸⁹ Zr-Labeled Single-Chain VEGF Mutants. Journal of Nuclear Medicine, 2016, 57, 1811-1816. | 5.0 | 21 |
| 227 | Clinical Potential of Human Epidermal Growth Factor Receptor 2 and Human Epidermal Growth Factor Receptor 3 Imaging in Breast Cancer. PET Clinics, 2018, 13, 423-435. | 3.0 | 21 |
| 228 | Harnessing Androgen Receptor Pathway Activation for Targeted Alpha Particle Radioimmunotherapy of Breast Cancer. Clinical Cancer Research, 2019, 25, 881-891. | 7.0 | 21 |
| 229 | Inhibiting cancer metabolism by aromatic carbohydrate amphiphiles that act as antagonists of the glucose transporter GLUT1. Chemical Science, 2020, 11, 3737-3744. | 7.4 | 21 |
| 230 | Imaging Tumor-Infiltrating Lymphocytes in Brain Tumors with [64Cu]Cu-NOTA-anti-CD8 PET. Clinical Cancer Research, 2021, 27, 1958-1966. | 7.0 | 21 |
| 231 | Molecular Imaging of Neuroendocrine Prostate Cancer by Targeting Delta-Like Ligand 3. Journal of Nuclear Medicine, 2022, 63, 1401-1407. | 5.0 | 21 |
| 232 | Diphosphine bifunctional chelators for low-valent metal ions. Crystal structures of the copper(I) complexes [CuClL12] and [CuL12][PF6] [L1â€=â€2,3-bis(diphenylphosphino)maleic anhydride]. Journal of the Chemical Society Dalton Transactions, 1997, , 855-862. | 2 1.1 | 20 |
| 233 | Utilization of metabolic, transport and receptor-mediated processes to deliver agents for cancer diagnosis. Advanced Drug Delivery Reviews, 1999, 37, 189-211. | 13.7 | 20 |
| 234 | Reproducibility and Repeatability of Semiquantitative ¹⁸ F-Fluorodihydrotestosterone Uptake Metrics in Castration-Resistant Prostate Cancer Metastases: A Prospective Multicenter Study. Journal of Nuclear Medicine, 2018, 59, 1516-1523. | 5.0 | 20 |

| # | Article | IF | CITATIONS |
|-----|---|------|-----------|
| 235 | A High-Denticity Chelator Based on Desferrioxamine for Enhanced Coordination of Zirconium-89. Inorganic Chemistry, 2020, 59, 11715-11727. | 4.0 | 20 |
| 236 | Rhenium complex of a triply deprotonated chelated thiosemicarbazide and its conversion to a nitride complex via a hydrazide intermediate. Crystal structure of [ReCl2(NH)(NHNH2)(PPh3)2]. Journal of the Chemical Society Dalton Transactions, 1995, , 1357. | 1.1 | 19 |
| 237 | Toward the Optimization of Click-Mediated Pretargeted Radioimmunotherapy. Molecular Pharmaceutics, 2019, 16, 2259-2263. | 4.6 | 19 |
| 238 | HER2-Targeted PET Imaging and Therapy of Hyaluronan-Masked HER2-Overexpressing Breast Cancer. Molecular Pharmaceutics, 2020, 17, 327-337. | 4.6 | 19 |
| 239 | pHLIP ICG for delineation of tumors and blood flow during fluorescence-guided surgery. Scientific Reports, 2020, 10, 18356. | 3.3 | 19 |
| 240 | Comparison of 68Ga-DOTA-JR11 PET/CT with dosimetric 177Lu-satoreotide tetraxetan (177Lu-DOTA-JR11) SPECT/CT in patients with metastatic neuroendocrine tumors undergoing peptide receptor radionuclide therapy. European Journal of Nuclear Medicine and Molecular Imaging, 2020, 47, 3047-3057. | 6.4 | 19 |
| 241 | Chemical tools for epichaperome-mediated interactome dysfunctions of the central nervous system. Nature Communications, 2021, 12, 4669. | 12.8 | 19 |
| 242 | Radioimmunotherapy Targeting Delta-like Ligand 3 in Small Cell Lung Cancer Exhibits Antitumor Efficacy with Low Toxicity. Clinical Cancer Research, 2022, 28, 1391-1401. | 7.0 | 19 |
| 243 | Radiopharmaceuticals for targeted radiotherapy of cancer. Expert Opinion on Therapeutic Patents, 2000, 10, 1057-1069. | 5.0 | 18 |
| 244 | The synthesis and evaluation of N1-(4-(2-[18F]-fluoroethyl)phenyl)-N8-hydroxyoctanediamide ([18F]-FESAHA), A PET radiotracer designed for the delineation of histone deacetylase expression in cancer. Nuclear Medicine and Biology, 2011, 38, 683-696. | 0.6 | 18 |
| 245 | Multinuclear NMR and MRI Reveal an Early Metabolic Response to mTOR Inhibition in Sarcoma. Cancer Research, 2017, 77, 3113-3120. | 0.9 | 18 |
| 246 | Acute Statin Treatment Improves Antibody Accumulation in EGFR- and PSMA-Expressing Tumors. Clinical Cancer Research, 2020, 26, 6215-6229. | 7.0 | 18 |
| 247 | First-in-Human Trial of Epichaperome-Targeted PET in Patients with Cancer. Clinical Cancer Research, 2020, 26, 5178-5187. | 7.0 | 18 |
| 248 | Radiometal-Labeled Somatostatin Analogs for Applications in Cancer Imaging and Therapy. Methods in Molecular Biology, 2007, 386, 227-240. | 0.9 | 18 |
| 249 | Radiosynthesis of the iodineâ€124 labeled Hsp90 inhibitor PUâ€H71. Journal of Labelled Compounds and Radiopharmaceuticals, 2016, 59, 129-132. | 1.0 | 17 |
| 250 | Molecular Imaging of Ovarian Cancer. Journal of Nuclear Medicine, 2016, 57, 827-833. | 5.0 | 17 |
| 251 | Imaging EGFR and HER3 through 89Zr-labeled MEHD7945A (Duligotuzumab). Scientific Reports, 2018, 8, 9043. | 3.3 | 17 |
| 252 | PET imaging of hypoxia. The Quarterly Journal of Nuclear Medicine: Official Publication of the Italian Association of Nuclear Medicine (AIMN) [and] the International Association of Radiopharmacology (IAR), 2001, 45, 183-8. | 0.5 | 17 |

| # | Article | IF | CITATIONS |
|-----|--|------|-----------|
| 253 | Delta-like ligand 3–targeted radioimmunotherapy for neuroendocrine prostate cancer. Proceedings of the National Academy of Sciences of the United States of America, 2022, 119, . | 7.1 | 17 |
| 254 | Evaluation of a bromine-76-labeled progestin 16α,17α-dioxolane for breast tumor imaging and radiotherapy: in vivo biodistribution and metabolic stability studies. Nuclear Medicine and Biology, 2008, 35, 655-663. | 0.6 | 16 |
| 255 | Acid specific dark quencher QC1 pHLIP for multi-spectral optoacoustic diagnoses of breast cancer. Scientific Reports, 2019, 9, 8550. | 3.3 | 16 |
| 256 | Design and preclinical evaluation of nanostars for the passive pretargeting of tumor tissue. Nuclear Medicine and Biology, 2020, 84-85, 63-72. | 0.6 | 16 |
| 257 | Production of Non-standard PET Radionuclides and the Application of Radiopharmaceuticals Labeled with these Nuclides. , 2007, , 159-181. | | 16 |
| 258 | The preparation of rhenium(V) oxo and imido complexes with Et2NCSNHCOPh and Et2NCSBC(NH)Ph. The x-ray crystal structure of [ReOCl(PhCONCSNEt2)2]. Polyhedron, 1993, 12, 221-225. | 2.2 | 15 |
| 259 | Synthesis and characterization of the copper(ii) complexes of new N2S2-donor macrocyclic ligands: synthesis and in vivo evaluation of the64Cu complexes. Dalton Transactions, 2009, , 177-184. | 3.3 | 15 |
| 260 | Comparison of Methods for Surface Modification of Barium Titanate Nanoparticles for Aqueous Dispersibility: Toward Biomedical Utilization of Perovskite Oxides. ACS Applied Materials & Interfaces, 2020, 12, 51135-51147. | 8.0 | 15 |
| 261 | Oncology-Inspired Treatment Options for COVID-19. Journal of Nuclear Medicine, 2020, 61, 1720-1723. | 5.0 | 15 |
| 262 | 89Zr-PET imaging of DNA double-strand breaks for the early monitoring of response following α- and β-particle radioimmunotherapy in a mouse model of pancreatic ductal adenocarcinoma. Theranostics, 2020, 10, 5802-5814. | 10.0 | 15 |
| 263 | ImmunoPET Imaging of Pancreatic Tumors with 89Zr-Labeled Gold Nanoparticle–Antibody Conjugates. Molecular Imaging and Biology, 2021, 23, 84-94. | 2.6 | 15 |
| 264 | Bromination from the Macroscopic Level to the Tracer Radiochemical Level:76Br Radiolabeling of Aromatic Compounds via Electrophilic Substitution. Bioconjugate Chemistry, 2009, 20, 808-816. | 3.6 | 14 |
| 265 | Copper-64 Radiopharmaceuticals for Oncologic Imaging. PET Clinics, 2009, 4, 49-67. | 3.0 | 14 |
| 266 | A PET Imaging Strategy for Interrogating Target Engagement and Oncogene Status in Pancreatic Cancer. Clinical Cancer Research, 2019, 25, 166-176. | 7.0 | 14 |
| 267 | Polyclonal antibodies to xenogeneic endothelial cells induce apoptosis and block support of tumor growth in mice. Vaccine, 2003, 21, 2667-2677. | 3.8 | 13 |
| 268 | Polyazamacrocycle Ligands Facilitate ⁸⁹ Zr Radiochemistry and Yield ⁸⁹ Zr Complexes with Remarkable Stability. Inorganic Chemistry, 2020, 59, 17473-17487. | 4.0 | 13 |
| 269 | Applications of nuclear-based imaging in gene and cell therapy: Probe considerations. Molecular Therapy - Oncolytics, 2021, 20, 447-458. | 4.4 | 13 |
| 270 | Synthesis and evaluation of an 18 F-labeled pyrimidine-pyridine amine for targeting CXCR4 receptors in gliomas. Nuclear Medicine and Biology, 2016, 43, 606-611. | 0.6 | 12 |

| # | Article | IF | CITATIONS |
|-----|--|------|-----------|
| 271 | Applying ⁸⁹ Zr-Transferrin To Study the Pharmacology of Inhibitors to BET Bromodomain Containing Proteins. Molecular Pharmaceutics, 2016, 13, 683-688. | 4.6 | 12 |
| 272 | Leveraging PET to image folate receptor $\hat{I}\pm$ therapy of an antibody-drug conjugate. EJNMMI Research, 2018, 8, 87. | 2.5 | 12 |
| 273 | Improved synthesis of the bifunctional chelator <i>p</i> -SCN-Bn-HOPO. Organic and Biomolecular Chemistry, 2019, 17, 6866-6871. | 2.8 | 12 |
| 274 | Multimodality labeling strategies for the investigation of nanocrystalline cellulose biodistribution in a mouse model of breast cancer. Nuclear Medicine and Biology, 2020, 80-81, 1-12. | 0.6 | 12 |
| 275 | Demarcation of Sepsis-Induced Peripheral and Central Acidosis with pH (Low) Insertion Cycle Peptide. Journal of Nuclear Medicine, 2020, 61, 1361-1368. | 5.0 | 12 |
| 276 | Sandmeyer reaction repurposed for the site-selective, non-oxidizing radioiodination of fully-deprotected peptides: Studies on the endogenous opioid peptide α-neoendorphin. Bioorganic and Medicinal Chemistry Letters, 2013, 23, 4347-4350. | 2.2 | 11 |
| 277 | ImmunoPET of Ovarian and Pancreatic Cancer with AR9.6, a Novel MUC16-Targeted Therapeutic Antibody. Clinical Cancer Research, 2022, 28, 948-959. | 7.0 | 11 |
| 278 | PET Imaging of Acidic Tumor Environment With 89Zr-labeled pHLIP Probes. Frontiers in Oncology, 2022, 12, . | 2.8 | 11 |
| 279 | An improved strategy for the synthesis of [18F]-labeled arabinofuranosyl nucleosides. Nuclear Medicine and Biology, 2012, 39, 1182-1188. | 0.6 | 10 |
| 280 | Dosimetry of 18F-Labeled Tyrosine Kinase Inhibitor SKI-249380, a Dasatinib-Tracer for PET Imaging. Molecular Imaging and Biology, 2012, 14, 25-31. | 2.6 | 10 |
| 281 | Fully-automated synthesis of 16β- 18 F-fluoro-5α-dihydrotestosterone (FDHT) on the ELIXYS radiosynthesizer. Applied Radiation and Isotopes, 2015, 103, 9-14. | 1.5 | 10 |
| 282 | Fully automated synthesis of [¹⁸ F]fluoroâ€dihydrotestosterone ([¹⁸ F]FDHT) using the FlexLab module. Journal of Labelled Compounds and Radiopharmaceuticals, 2016, 59, 424-428. | 1.0 | 10 |
| 283 | Assessment of Simplified Methods for Quantification of 18F-FDHT Uptake in Patients with Metastatic Castration-Resistant Prostate Cancer. Journal of Nuclear Medicine, 2019, 60, 1221-1227. | 5.0 | 10 |
| 284 | A Molecularly Targeted Intraoperative Near-Infrared Fluorescence Imaging Agent for High-Grade Serous Ovarian Cancer. Molecular Pharmaceutics, 2020, 17, 3140-3147. | 4.6 | 10 |
| 285 | Manipulating the In Vivo Behaviour of 68Ga with Tris(Hydroxypyridinone) Chelators: Pretargeting and Blood Clearance. International Journal of Molecular Sciences, 2020, 21, 1496. | 4.1 | 10 |
| 286 | ERK Inhibition Improves Anti–PD-L1 Immune Checkpoint Blockade in Preclinical Pancreatic Ductal Adenocarcinoma. Molecular Cancer Therapeutics, 2021, 20, 2026-2034. | 4.1 | 10 |
| 287 | Fluorescence labeling of a NaV1.7-targeted peptide for near-infrared nerve visualization. EJNMMI Research, 2020, 10, 49. | 2.5 | 10 |
| 288 | Caveolin-1 temporal modulation enhances antibody drug efficacy in heterogeneous gastric cancer. Nature Communications, 2022, 13, 2526. | 12.8 | 10 |

| # | Article | IF | CITATIONS |
|-----|--|-----|-----------|
| 289 | Pretargeted PET of Osteodestructive Lesions in Dogs. Molecular Pharmaceutics, 2022, 19, 3153-3162. | 4.6 | 10 |
| 290 | Synthesis and evaluation of 18F-labeled ATP competitive inhibitors of topoisomerase II as probes for imaging topoisomerase II expression. European Journal of Medicinal Chemistry, 2014, 86, 769-781. | 5.5 | 9 |
| 291 | Influence of free fatty acids on glucose uptake in prostate cancer cells. Nuclear Medicine and Biology, 2014, 41, 254-258. | 0.6 | 9 |
| 292 | Long–Half-Life ⁸⁹ Zr-Labeled Radiotracers Can Guide Percutaneous Biopsy Within the PET/CT Suite Without Reinjection of Radiotracer. Journal of Nuclear Medicine, 2018, 59, 399-402. | 5.0 | 9 |
| 293 | Aromatic carbohydrate amphiphile disrupts cancer spheroids and prevents relapse. Nanoscale, 2020, 12, 19088-19092. | 5.6 | 8 |
| 294 | Imaging of Cancer Î ³ -Secretase Activity Using an Inhibitor-Based PET Probe. Clinical Cancer Research, 2021, 27, 6145-6155. | 7.0 | 8 |
| 295 | Functionalised copper-64 complexes as precursors of potential PET imaging agents for neurodegenerative disorders. New Journal of Chemistry, 2009, 33, 1845. | 2.8 | 7 |
| 296 | Ex vivo sentinel lymph node mapping in laparoscopic resection of colon cancer. Colorectal Disease, 2011, 13, 1249-1255. | 1.4 | 7 |
| 297 | Antibody-Targeted Imaging of Gastric Cancer. Molecules, 2020, 25, 4621. | 3.8 | 7 |
| 298 | Synthesis and Comparative <i>In Vivo</i> Evaluation of Site-Specifically Labeled Radioimmunoconjugates for DLL3-Targeted ImmunoPET. Bioconjugate Chemistry, 2021, 32, 1255-1262. | 3.6 | 7 |
| 299 | "Friction by Definitionâ€: Conflict at Patient Handover Between Emergency and Internal Medicine Physicians at an Academic Medical Center. Western Journal of Emergency Medicine, 2021, 22, 1227-1239. | 1.1 | 7 |
| 300 | Harnessing the Bioorthogonal Inverse Electron Demand Diels-Alder Cycloaddition for Pretargeted PET Imaging. Journal of Visualized Experiments, 2015, , e52335. | 0.3 | 6 |
| 301 | Imaging Early-Stage Metastases Using an 18F-Labeled VEGFR-1-Specific Single Chain VEGF Mutant. Molecular Imaging and Biology, 2021, 23, 340-349. | 2.6 | 6 |
| 302 | Predicting CAR-T cell Immunotherapy Success through ImmunoPET. Clinical Cancer Research, 2021, 27, 911-912. | 7.0 | 6 |
| 303 | Antilipolytic drug boosts glucose metabolism in prostate cancer. Nuclear Medicine and Biology, 2013, 40, 524-528. | 0.6 | 5 |
| 304 | Leveraging synthetic chlorins for bio-imaging applications. Chemical Communications, 2020, 56, 12608-12611. | 4.1 | 5 |
| 305 | Radiopharmacologic screening of antibodies to the unshed ectodomain of MUC16 in ovarian cancer identifies a lead candidate for clinical translation. Nuclear Medicine and Biology, 2020, 86-87, 9-19. | 0.6 | 5 |
| 306 | First-in-Humans Trial of Dasatinib-Derivative Tracer for Tumor Kinase-Targeted PET. Journal of Nuclear Medicine, 2020, 61, 1580-1587. | 5.0 | 5 |

| # | Article | IF | CITATIONS |
|-----|---|-----------|-----------|
| 307 | Influence of Fc Modifications and IgG Subclass on Biodistribution of Humanized Antibodies Targeting L1CAM. Journal of Nuclear Medicine, 2022, 63, 629-636. | 5.0 | 5 |
| 308 | EGFR-Targeted ImmunoPET of UMUC3 Orthotopic Bladder Tumors. Molecular Imaging and Biology, 2022, 24, 511-518. | 2.6 | 5 |
| 309 | pHâ€Responsive Polymers for Improving the Signalâ€ŧoâ€Noise Ratio of Hypoxia PET Imaging with [18 F]Fluoromisonidazole. Macromolecular Rapid Communications, 2020, 41, 2000061. | 3.9 | 4 |
| 310 | PET/CT Imaging with an 18F-Labeled Galactodendritic Unit in a Galectin-1–Overexpressing Orthotopic Bladder Cancer Model. Journal of Nuclear Medicine, 2020, 61, 1369-1375. | 5.0 | 4 |
| 311 | Immuno-PET Detects Changes in Multi-RTK Tumor Cell Expression Levels in Response to Targeted Kinase Inhibition. Journal of Nuclear Medicine, 2021, 62, 366-371. | 5.0 | 4 |
| 312 | Exploiting the MUC5AC Antigen for Noninvasive Identification of Pancreatic Cancer. Journal of Nuclear Medicine, 2021, 62, 1384-1390. | 5.0 | 4 |
| 313 | Copperâ€64/61 and iodineâ€125â€labeled dotaâ€DTYR ¹ â€octreotate: A new somatostatin analog f labeling with metals and halogens. Journal of Labelled Compounds and Radiopharmaceuticals, 2001, 44, S948. | or 1.0 | 3 |
| 314 | Bimodal Imaging of Mouse Peripheral Nerves with Chlorin Tracers. Molecular Pharmaceutics, 2021, 18, 940-951. | 4.6 | 3 |
| 315 | 3D-Printable Platform for High-Throughput Small-Animal Imaging. Journal of Nuclear Medicine, 2020, 61, 1691-1692. | 5.0 | 3 |
| 316 | Noninvasive Imaging of CD4+ T Cells in Humanized Mice. Molecular Cancer Therapeutics, 2022, 21, 658-666. | 4.1 | 3 |
| 317 | Radiopharmaceuticals for Imaging in Oncology with Special Emphasis on Positron-Emitting Agents. , 2013, , 35-78. | | 2 |
| 318 | Molecular Imaging Companion Diagnostics. , 2019, , 201-228. | | 2 |
| 319 | Technical Note: Patientâ€morphed meshâ€ŧype phantoms to support personalized nuclear medicine dosimetry — a proof of concept study. Medical Physics, 2021, 48, 2018-2026. | 3.0 | 2 |
| 320 | Novel Tracers and Radionuclides in PET Imaging. Radiologic Clinics of North America, 2021, 59, 887-918. | 1.8 | 2 |
| 321 | Radiolabeled Antibodies for Tumor Imaging and Therapy. , 2005, , 685-714. | | 1 |
| 322 | ⁶⁴ Cuâ€₱TSM as an inhibitor of tumor recurrence. Journal of Labelled Compounds and Radiopharmaceuticals, 2001, 44, S87. | 1.0 | 0 |
| 323 | Preface: 14th International Workshop on Targetry and Target Chemistry (WTTC). , 2012, , . | | 0 |
| 324 | Precision Medicine…Visualized—a Message from the President of the WMIC. Molecular Imaging and Biology, 2015, 17, 443-444. | 2.6 | 0 |

| # | Article | IF | CITATIONS |
|-----|--|-----|-----------|
| 325 | Emerging Radiopharmaceuticals in Clinical Oncology. , 2016, , 1-43. | | Ο |
| 326 | The 2019 World Molecular Imaging Congress (WMIC) and Molecular Imaging and Biology (MIB) Awards. Molecular Imaging and Biology, 2020, 22, 6-8. | 2.6 | 0 |
| 327 | Changing of the Guard at Molecular Imaging & Biology. Molecular Imaging and Biology, 2020, 22, 1-3. | 2.6 | 0 |
| 328 | Antibody-Based Molecular Imaging. , 2021, , 547-562. | | 0 |
| 329 | REPLY TO LETTER TO THE EDITOR: POTENTIAL USE OF RADIOLABELED ANTIBODIES FOR IMAGING AND TREATMENT OF COVID-19. Journal of Nuclear Medicine, 2021, 62, jnumed.121.261950. | 5.0 | 0 |
| 330 | State-of-the-Art of Radiometal-based Bioconjugates for Molecular Imaging and Radiotherapy. Bioconjugate Chemistry, 2021, 32, 1175-1176. | 3.6 | 0 |
| 331 | SU-GG-J-03: 3D Pathology Validation for Head-And-Neck Tumor Segmentation in PET/CT/MRI Images. Medical Physics, 2008, 35, 2679-2679. | 3.0 | 0 |
| 332 | Novel Positron Emitting Radiopharmaceuticals. , 2016, , 1-43. | | 0 |
| 333 | Novel Positron-Emitting Radiopharmaceuticals. , 2017, , 129-171. | | 0 |